

1-6-2023

## Identification of TP53 mutations in circulating tumour DNA in high grade serous ovarian carcinoma using next generation sequencing technologies

Leslie Calapre  
*Edith Cowan University*

Tindaro Giardina

Aaron B. Beasley  
*Edith Cowan University, a.beasley@ecu.edu.au*

Anna L. Reid  
*Edith Cowan University, anna.reid@ecu.edu.au*

Colin Stewart

*See next page for additional authors*

Follow this and additional works at: <https://ro.ecu.edu.au/ecuworks2022-2026>



Part of the [Oncology Commons](#)

---

10.1038/s41598-023-27445-2

Calapre, L., Giardina, T., Beasley, A. B., Reid, A. L., Stewart, C., Amanuel, B., ... & Gray, E. S. (2023). Identification of TP53 mutations in circulating tumour DNA in high grade serous ovarian carcinoma using next generation sequencing technologies. *Scientific Reports*, 13, Article 278. <https://doi.org/10.1038/s41598-023-27445-2>

This Journal Article is posted at Research Online.  
<https://ro.ecu.edu.au/ecuworks2022-2026/1893>

---

**Authors**

Leslie Calapre, Tindaro Giardina, Aaron B. Beasley, Anna L. Reid, Colin Stewart, Benhur Amanuel, Tarek M. Meniawy, and Elin S. Gray



OPEN

## Identification of TP53 mutations in circulating tumour DNA in high grade serous ovarian carcinoma using next generation sequencing technologies

Leslie Calapre<sup>1</sup>, Tindaro Giardina<sup>2</sup>, Aaron B. Beasley<sup>1,3</sup>, Anna L. Reid<sup>1,3</sup>, Colin Stewart<sup>2,4</sup>, Benhur Amanuel<sup>1,2,4</sup>, Tarek M. Meniawy<sup>1,4,5</sup> & Elin S. Gray<sup>1,2</sup>✉

Plasma circulating tumour DNA (ctDNA) has been suggested to be a viable biomarker of response to treatment in patients with high grade serous ovarian carcinoma (HGSOC). *TP53* mutations are present in more than 90% of HGSOCs but somatic variants are distributed across all exonic regions of the gene, requiring next generation sequencing (NGS) technologies for mutational analysis. In this study, we compared the suitability of the Accel (Swift) and Oncomine (ThermoFisher) panels for identification of *TP53* mutations in ctDNA of HGSOC patients (N = 10). Only 6 patients (60%) were found to have *TP53* mutations using the ACCEL panel but the addition of molecular tags in the Oncomine panel improved ctDNA detection with at least one mutation detected in all cases (100%). Orthogonal validation of the 14 somatic variants found by Oncomine, using droplet digital PCR, confirmed 79% (11/14) of the identified mutations. Overall, the Oncomine panel with unique molecular identifiers (UMI) appears more useful for ctDNA analysis in HGSOC.

High-grade serous ovarian carcinoma (HGSOC) is the most common subtype of primary tubo-ovarian malignancy, accounting for approximately 70% of cases overall. Most cases present at advanced stage with peritoneal spread and often lymph node and/or distant metastasis. The serum glycoprotein cancer antigen 125 (CA-125) is a commonly used diagnostics biomarker in the investigation of patients presenting with possible ovarian neoplasia and for monitoring treatment response<sup>1,2</sup>. However, while CA-125 can indicate the trend of treatment response, it does not directly reflect absolute tumour volume<sup>3</sup>. Furthermore, it is limited by specificity, intra-tumoural and inter-patient heterogeneity and a long biological half-life in serum. Thus, a more sensitive and specific biomarker would be helpful in the management of HGSOC patients.

Recent studies have suggested that serum DNA-based biomarkers may have superior capabilities for reflecting tumour burden and measuring treatment response in cancer patients. In contrast to protein biomarkers, which typically are not specific to cancer cells, circulating tumour DNA (ctDNA) measures levels of mutations in plasma cell-free DNA, providing cancer-specific information. Plasma ctDNA fragments have a short half-life, and their levels have been shown in other cancer types to be related to tumour volume and response to treatment<sup>4,5</sup>. Thus, ctDNA appears to be a potentially useful adjunct biomarker in oncology.

More than 90% of patients with HGSOC have been shown to harbour mutations in the *TP53* gene<sup>6–8</sup>. Earlier studies have shown that *TP53* mutations can be detected in ctDNA from patients with advanced stage HGSOC and that, in a small number of patients studied, changes in ctDNA levels correlated with clinical response and outperformed CA-125<sup>9–12</sup>. However, *TP53* mutations in HGSOC are randomly distributed in all coding regions and chemotherapy has been shown to impose clonal evolution of *TP53* mutations; the resulting potential contraction or expansion of mutant clones therefore poses a challenge for patient surveillance during treatment. Thus, ctDNA analysis in HGSOC is likely to require next generation sequencing (NGS) technologies.

<sup>1</sup>School of Medical and Health Sciences, Edith Cowan University, Joondalup, WA, Australia. <sup>2</sup>Anatomical Pathology, PathWest Laboratory Medicine, QEII Medical Centre, Nedlands, WA, Australia. <sup>3</sup>Centre for Precision Health, Edith Cowan University, Joondalup, WA, Australia. <sup>4</sup>Medical School, University of Western Australia, Crawley, WA, Australia. <sup>5</sup>Department of Medical Oncology, Sir Charles Gairdner Hospital, Nedlands, WA, Australia. ✉email: e.gray@ecu.edu.au

In this study, we directly compared two NGS platforms to identify *TP53* mutations in plasma ctDNA of HGSOC patients. We demonstrate the impact of unique molecular identifiers (UMI) and an efficient bioinformatics pipeline for improved sensitivity of NGS-based *TP53* profiling.

## Materials and methods

**Patients.** We collected blood samples from 10 stage III and IV HGSOC patients with active disease enrolled for study in 2018 at Western Oncology Clinic and Sir Charles Gairdner Hospital (SCGH) in Perth, Western Australia. Written informed consent was obtained from all patients, and procedures were approved by the Human Research Ethics Committees from Edith Cowan University (No. 11543) and Sir Charles Gairdner Hospital (No. 2013-246) in compliance with Helsinki Declaration. Experiments were conducted per institutional and national guidelines and regulations.

**Tissue analysis.** Tumour tissue from primary or interval debulking surgery was used for sequence analysis. Hematoxylin and eosin (H&E)-stained sections were assessed by a pathologist and the percentage of tumour cells estimated. Microdissection was performed when the neoplastic cell content was below 50%. DNA was isolated using QIAamp Tissue Formalin-Fixed Paraffin-Embedded (FFPE) Kits (Qiagen, Hilden, Germany) as per the manufacturer's instructions. FFPE genomic DNA (gDNA) was stored at 4 °C until processed for targeted sequencing.

**Plasma samples preparation and cell-free DNA (cfDNA) extractions.** Blood samples from stage four HGSOC were collected in EDTA vacutainer or Cell-Free DNA BCT (Streck, La Vista, NE) tubes and stored at 4 °C. Plasma was separated within 24 h by centrifugation at 300×g for 20 min, followed by a second centrifugation at 4700×g for 10 min and then stored at –80 °C until extraction. cfDNA was isolated from 5 ml of plasma using QIAamp Circulating Nucleic Acid Kits (Qiagen, Hilden, Germany) as per the manufacturer's instructions. Plasma cfDNA was eluted in 40 µl AVE buffer (Qiagen, Hilden, Germany) and stored at –80 °C until analysis.

**Accel comprehensive TP53 assay library preparation and sequencing.** DNA derived from FFPE tumour tissue (N=10) and plasma samples (N=10) underwent NGS. Matched non-neoplastic control tissue was examined in 5 patients to further delineate true somatic mutations from sequencing artefacts. DNA samples were amplified using a highly-multiplexed polymerase chain reaction (PCR) that amplifies 21 exonic regions of *TP53* alone using the ACCEL-Amplicon *TP53* Comprehensive Panel (Swift Biosciences). Forward and reverse strand NGS libraries were prepared according to the manufacturer's instructions. In brief, forward and reverse oligonucleotide pools were hybridised to DNA samples overnight. Hybridised samples were then ligated, extended, and amplified with unique index sequences (barcodes) and sequencing adaptors. Amplified libraries were purified using Agencourt AMPure XP magnetic beads (Beckman Coulter, Brea, CA, USA), first at a ratio of 1 (library):1 (beads), as per the manufacturer's protocol, followed by a second round of purification at a library to bead ratio of 1.25:1. Library DNA concentrations were quantified using a Qubit 3.0 fluorometer. Libraries were normalized to 4 nmol/l in EBT buffer, pooled, and sequenced on a MiSeq instrument (Illumina, San Diego, CA, USA). Sequence alignment and variant calling was performed using the Erase-Seq bioinformatics pipeline through collaboration with Fluxion. Variants with allele frequency (VAF) > 3% and ≥ 0.2% in tissue and cfDNA respectively were considered true mutations.

**Oncomine assay library preparation, sequencing and bioinformatics.** Plasma cfDNA derived from 10 plasma samples underwent library preparation. DNA samples were amplified using highly multiplexed PCR that amplifies 17 exonic regions of *TP53* and 135 hotspots in nine genes (*AKT1*, *EGFR*, *ERBB2*, *ERBB3*, *ESR1*, *FBXW7*, *KRAS*, *PIK3CA*, *SF3B1*), and copy numbers in three genes (*CCND1*, *ERBB2*, *FGFR1*) commonly mutated in breast cancer. Sequencing libraries were created using the Oncomine Breast cfDNA v2 assay (Thermo Fisher), subjected to emulsion PCR, and sequencing templates were prepared in the Ion Chef (Thermo Fisher) using the Ion 530 Kit-Chef (Thermo Fisher). Five different barcoded libraries were pooled and loaded onto one Ion 530 chip (Thermo Fisher) to obtain appropriate coverage. Sequencing was carried out using an Ion S5 sequencer (Thermo Fisher). Each Ion 530 chip produced approximately 18 million reads. Reads underwent primary analysis using the Ion Reporter 5.10.5.0, which includes quality control, read trimming, and mapping to the human genome (hg19). The threshold for identification of true somatic variants was based on unique molecular identifiers (UMI). Variants are considered true mutations if they have a total molecular coverage ≥ 1000 and allele molecular coverage (AMC) of ≥ 1.

**Droplet digital PCR (ddPCR).** Commercially available and/or customized *TP53* probes were used to analyse ctDNA by ddPCR. Droplets were generated using an Automatic Droplet generator QX200 AutoDG (Bio-Rad, Hercules, CA). Amplifications were performed using cycling conditions previously described<sup>13</sup>.

**Statistics.** Pearson correlation was employed to determine the correlation between allele molecular coverage (ONCOMINE) and copies per 20 µl reaction (ddPCR). Statistical analyses were performed using GraphPad Prism version 5.

## Results

**Identification of TP53 mutations in tissue.** We first identified single nucleotide variations (SNVs) in *TP53* from tumour tissue. The mutations identified in the tissue served as a guide for the identification of SNVs in plasma cfDNA. The ACCEL-Amplicon TP53 Comprehensive Panel (Accel) was used for mutational profiling in the tissue as it provided comprehensive exonic coverage of the *TP53* gene. Ten tissue samples with confirmed HGSOc were analysed. In addition, five adjacent samples of non-neoplastic tissue were included as negative controls. Each tissue sample in this study was sequenced to at least 1000× coverage, with a median coverage of 15,000× (range 1000×–25,000×). We found a total of 13 SNVs in *TP53* in 8 of the 10 tumours analysed (80%). The mutations and corresponding frequency abundance are summarised in Table S1.

**Comparison of NGS panel for TP53 analysis in ctDNA.** We next compared the efficiency of the Accel panel to the OncoPrint Breast cfDNA Assay V2 (OncoPrint) for ctDNA detection in HGSOc. Comparison of the technical specification between OncoPrint and Accel are detailed in Table S2. Mutations identified using these panels are also summarised in Table S1.

Using the Accel panel, plasma ctDNA was sequenced to a median coverage of 33,563× (Table S1), ranged between 1000 and 62,081× (Table S1). Nine SNVs were identified across 21 loci of *TP53* (Table S1) in 6 out of 10 patients (60%), using the Erase-Seq bioinformatics pipeline. The pipeline has a limit of detection (LOD) of 0.2% and the fractional abundance (FA) of the mutations identified via the Accel NGS panel ranged from 0.2 to 3% (Table S1). Only three patients (OC1, OC4 and OC10) had one concordant mutation between plasma ctDNA and tissue biopsy. In the other 7 patients, *TP53* mutations were found at relatively high frequency in plasma but these were not confirmed in the tissue (Fig. S2).

Overall sequence coverage using the OncoPrint panel ranged between 21,021× and 153,440×, with a median coverage of 69,773 (Table S1). In addition, the molecular coverage of each locus was ≥ 1000× in all plasma ctDNA analysed. A total of 21 SNVs were found in all 10 patients (Fig. S1), which ranged from 0.03 to 0.86% FA (Table 1). Out of the 21 SNVs identified in plasma, only four mutations; p.R282G, p.I195T, p.R248Q and p.R273C from OC1, OC3, OC4 and OC10 respectively, were also found in the tissue (Table S1). Three of these four mutations were also detected by the Accel panel in the plasma. Overall, there was a low concordance (28%) in the mutational profile obtained between plasma ctDNA and tissue. In one patient (OC7), the OncoPrint panel also identified a *KRAS* p.G12D mutation in addition to *TP53* mutations. The *KRAS* gene is mutated in 14% of ovarian cancers, commonly in codon G12 (41%, COSMIC).

We also compared the mutations identified in ctDNA by Accel and OncoPrint (Table 1). We found four *TP53* mutations, which ranged from 0.2 to 0.8% allele frequency, in the plasma of 4 different HGSOc patients via the Accel and OncoPrint sequencing panels (Fig. 1a). In addition, there were 11 plasma mutations (range: 0.03% to

Patient ID	Gene	Mutation	Chromosomal position	OncoPrint panel	Accel comprehensive TP53 panel	ddPCR validation
OC1	<i>TP53</i>	p.R282G	17:7,577,094	<b>0.54%</b>	<b>0.3%</b>	<b>0.7%</b>
		p.G266R	17:7,577,142	0.03% <sup>a</sup>	–	0.02%
OC2	<i>TP53</i>	p.R273H	17:7,577,120	0.04%	–	–
OC3	<i>TP53</i>	p.I195T	17:7,578,265	0.03% <sup>a</sup>	–	0.03%
	<i>TP53</i>	p.N13N	17:7,579,757	<sup>b</sup>	0.2%	–
OC4	<i>TP53</i>	p.R282W	17:7,577,094	0.10%	–	0.7%
		p.R273L	17:7,577,120	0.10%	–	–
		p.R248Q	17:7,577,538	<b>0.86%</b>	<b>0.6%</b>	<b>0.50%</b>
		p.C238Y	17:7,577,568	0.38%	–	0.10%
		p.Y220C	17:7,578,190	0.28%	–	0.25%
		p.R280S	17:7,577,100	<b>2%</b>	<b>3%</b>	<b>3%</b>
OC5	<i>TP53</i>	p.T253P	17:7,577,524	–	0.3%	–
		p.R282W	17:7,577,094	0.04%	–	0.04%
		p.I195T	17:7,578,265	<b>0.86%</b>	<b>0.7%</b>	<b>0.83%</b>
OC6		p.G266R	17:7,577,142	0.04%	–	0.11%
OC7	<i>TP53</i>	p.S378fs	17:7,572,976	0.08%	–	<sup>c</sup>
OC8	<i>TP53</i>	p.R196Q	17:7,578,262	0.29%	–	<sup>c</sup>
		p.S185G	17:7,578,377	–	0.2%	–
		p.D184H	17:7,578,380	–	0.2%	–
OC9	<i>TP53</i>	p.Y234C	17:7,577,580	0.04%	–	–
OC10	<i>TP53</i>	p.R273C	17:7,577,121	<b>0.25%</b>	<b>0.27%</b>	<b>0.58%</b>

**Table 1.** Somatic mutations identified in ctDNA using the ONCOMINE and ACCEL NGS panels and validated by ddPCR. Bold denotes concordant variants identified using the Accel and OncoPrint in cfDNA that were confirmed by ddPCR. Italics denotes variants found in OncoPrint or Accel that are confirmed via orthogonal validation using ddPCR. <sup>a</sup>Below threshold. <sup>b</sup>Not covered. <sup>c</sup>Not tested. –, not detected.

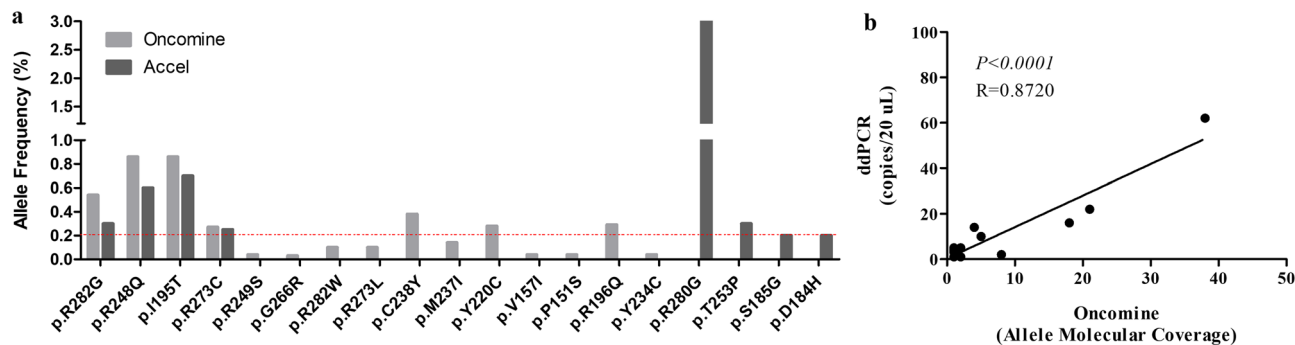


**Figure 1.** Comparison of SNVs identified via Accel vs Oncomine in the plasma of HGSCO patients. **(a)** Bar graph denotes the SNVs and corresponding allele frequency (%) that are found by both ONCOMINE and ACCEL, ONCOMINE alone or ACCEL alone. Red line denotes the limit of detection (LOD) for the Accel NGS panel. **(b)** Correlation of the number of mutant copies derived from NGS (Oncomine, UMI) and ddPCR. Analysis was performed using Pearson's correlation and  $P < 0.05$  is considered significant.

0.86% FA), detected by the Oncomine panel but not with Accel. Of note, 9 of the 11 mutations were below 0.2% allele frequency, the analytical threshold of the Accel panel. By contrast, there were four mutations (p.R280S, p.T253P, p.S185G and p.D184H) that were found above 0.2% allele frequency by the Accel sequencing panel but were not confirmed in the same plasma sample by Oncomine despite sufficient total and molecular coverage. Lastly, the region covering a silent N13N mutation found in ctDNA by the Accel panel in OC3 is not covered by the Oncomine panel.

**Orthogonal validation of SNVs identified using Accel or Oncomine.** We conducted orthogonal validation using ddPCR of 8 and 15 mutations identified by the Accel and Oncomine panels respectively, with four of these mutations found in both NGS platform. Only five of the 8 mutations (62.5%) identified by the Accel panel were confirmed by ddPCR, including the four mutations that were also detected by Oncomine (Table 1). By contrast, 12 of the 15 mutations (80%) found by Oncomine were confirmed by ddPCR, including 3 mutations that were deemed below the analytical threshold for Oncomine (0.03% FA).

Notably of the 12 mutations found by Oncomine and validated by ddPCR, the number of mutant copies found via NGS, which is indicated as the total AMC, was significantly concordant to the relative copies in the 8  $\mu$ l of ctDNA added to the ddPCR reaction ( $R = 0.8720$ ,  $P < 0.0001$ , Fig. 1b).

**TP53 mutations for ctDNA tracking.** We used TP53 mutations identified via NGS to monitor response in four patients in this cohort for whom we collected longitudinal samples throughout their treatment course. Plasma ctDNA were quantified using ddPCR and represented in each patient graph as copies per ml of plasma. Three of the four patients (OC3, OC4 and OC6) had received adjuvant treatment approximately 1 week after interval debulking surgery, whilst OC5 had neoadjuvant chemotherapy prior to surgery (Fig. 2, Table S3).

For patient OC3 (Fig. 2a), sub-optimal debulking surgery led to  $> 2$  cm residual disease and 12 months of maintenance with anti-VEGF therapy (Bevacizumab). Post-Bevacizumab the patient was well and without new symptoms from weeks 67–103, but increasing ctDNA levels eventually coincided with disease progression on radiological imaging (week 118). Similarly, patient OC4 (Fig. 2b), who had several rounds of chemotherapy had detectable ctDNA at week 142, which correlated with progressive disease in the pelvis, peritoneum and rectus abdominis that was confirmed by PET scan on week 144. Likewise, the longitudinal disease monitoring of patient OC6 (Fig. 2c) revealed detectable ctDNA levels post adjuvant chemotherapy, suggesting residual disease.

Patient OC5 (Fig. 2d) was treated with neoadjuvant chemotherapy prior to debulking surgery and maintenance Bevacizumab post-surgery. Detectable ctDNA levels between weeks 30–72 during maintenance anti-VEGF therapy appeared to indicate the presence of residual disease, culminating in the confirmation of disease progression in the peritoneum and lymph nodes at week 74. However, the decline in ctDNA at week 72, from week 36, was followed by apparent disease control by week 104, likely due to the Cisplatin/Doxil treatment.

## Discussion

Previous studies have shown that TP53 mutations are a potentially useful target for ctDNA analysis in patients with advanced HGSO<sup>9–12</sup>. However, somatic variants are distributed across all exonic regions of the gene. Thus, interrogation of the entire TP53 gene is required for comprehensive and accurate ctDNA analysis in these tumours. Herein, we compared two NGS platforms that are suitable for TP53 mutation identification in plasma ctDNA and demonstrated the impact of UMI for improved sensitivity of NGS-based TP53 mutational profiling.

Overall, our results appear to indicate that the low LOD of both Oncomine and Accel panels makes them suitable for TP53 mutational profiling in ctDNA of HGSO patients. All exonic regions of TP53 are represented in the Accel panel. However, reduction of the threshold to 0.2% required the use of customised analysis pipelines such as ERASE-Seq. By contrast, the addition of molecular tags in the Oncomine panel improved TP53 mutation detection allowing identification of SNVs at  $< 0.05\%$  frequency abundance. However, only 80% of the exonic regions of TP53 are covered and thus while the Oncomine panel appears to have superior detection

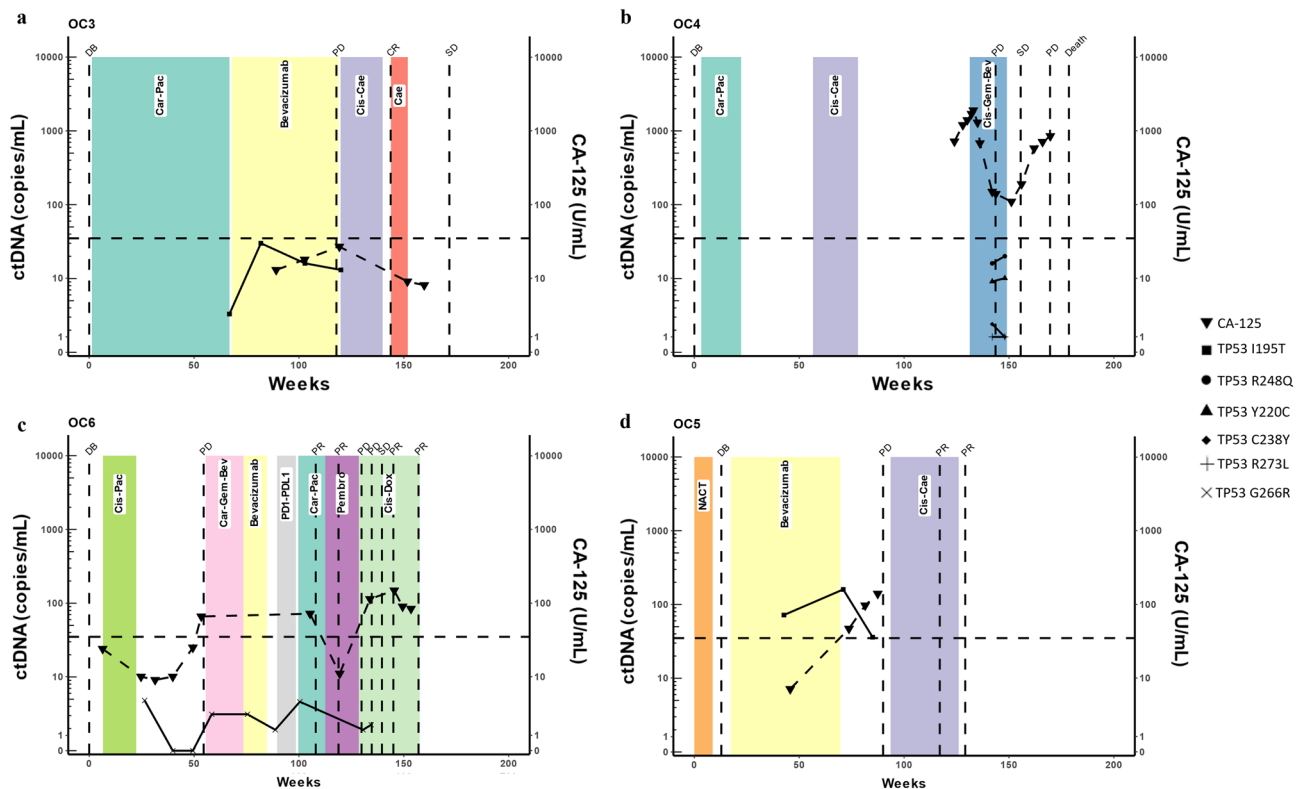


**Figure 2.** Longitudinal patient monitoring via *TP53* mutation in plasma ctDNA. (a–d) Line graph denotes the clinical status of four HGSOc patients that were longitudinally monitored throughout their disease course. ctDNA levels indicated by solid lines, different mutations indicated by changing point. CA-125 indicated by dashed line graph with upside-down triangles. Horizontal dashed line indicates the CA-125 positivity threshold of 35 units/mL of blood. Therapy time frames are indicated by coloured boxes with treatment noted in the centre. Vertical dashed lines indicate time of scans or surgery with the outcome named above the line. *PD* progressive disease, *SD* stable disease, *PR* partial response, *CR* complete response, *DB* debulking.

sensitivity than the Accel, it precludes identification of potential clinically relevant mutations in unrepresented exonic regions. Furthermore, there are a few limitations with amplicon sequencing over hybrid capture. First, tiling amplicons in one pool can lead to interactions reducing quality or requiring non-tiled amplicons reducing coverage. Splitting primers into two pools would overcome this but may reduce sensitivity for rare variants as found in ctDNA. Furthermore, mutations in the primer region may cause dropout of the amplicon. However, amplicon sequencing has several benefits including reduced cost, easier automation, less hands-on-time, and by virtue of the method have higher on-target rates compared to hybrid capture.

Mutational profiling through the use of a liquid biopsy is challenging due to the mainly low amounts of circulating ctDNA and the very low representation of mutated ctDNA molecules extractable from the blood plasma. Therefore, methods which are able to detect a small number of mutated molecules in an abundance of wild-type DNA fragments with high sensitivity and specificity are required<sup>14,15</sup>. The addition of UMI, random nucleotide sequences barcoding each DNA-fragment prior to PCR amplification, has been demonstrated to overcome the drawbacks of PCR-based NGS, including DNA polymerase errors and generation of PCR duplicates as a result of sequencing the same molecule multiple times<sup>16</sup>. This has led to the discovery of mutations at <0.1% FA which is within the typical range of ctDNA in plasma, especially in treated patients. Currently, quantitative PCR, amplification refractory mutation system (ARMS), digital PCR, beads, emulsion, amplification, and magnetics (BEAMing) and NGS are widely used<sup>17</sup>. While these methods enable a sensitive detection down to 0.01%, only NGS facilitates the parallel detection of a broader range of mutations by multi-gene or multi-target gene panels. In general, it appears as though ctDNA might be a better blood-based biomarker for monitoring patients compared to CA-125<sup>18</sup>. Similarly to our study, others have also utilised NGS with UMI barcoding and ddPCR for patient monitoring in HGSOc, similarly showing good correlations with changes in patient disease states<sup>19</sup>. In addition to mutation screening, other avenues of predicting patient response to therapy or disease progression may be through the use of somatic copy number alterations in ctDNA given the propensity of HGSOc to harbour them<sup>20</sup>.

One of the most critical aspects in analysing low VAF mutations in the plasma is the accumulation of somatic mutations to haematopoietic cells known as clonal haematopoiesis of indeterminate potential (CHIP), greatly increasing with age<sup>21</sup>. For example, the majority of healthy people aged over 50 have nonsynonymous mutations found both in matched cfDNA and blood cell DNA<sup>22</sup>, with *TP53* routinely detected as a CHIP-derived mutation<sup>21–24</sup>. This may be problematic in HGSOc ctDNA analysis due to the prevalence and non-hotspot nature

Patient	Stage	1st round chemotherapy (cycles)	Length of time* (weeks)	Concordant mutations in blood vs tissue (%)	Blood tube	Time to process (HH:MM)	Volume (ml)	Nearest CA-125 level (U/ml)
OC1 <sup>^</sup>	IIIa	Carboplatin/paclitaxel (1)	-4	1 (50%)	EDTA	3:44	5	-
OC2	III	Carboplatin/paclitaxel (6)	-14	0 (0%)	EDTA	5:11	5	-
OC3	IIIc	Carboplatin/paclitaxel (6)	-67	1 (50%)	EDTA	20:34	5	13
OC4	IIIc	Carboplatin/paclitaxel (6)	-142	1 (50%)	EDTA	3:12	5	142
OC5	IVa	Chemotherapy (Neoadj) (3)	-30	N/A (CR*)	EDTA	4:21	5	33
OC6	III	Cisplatin/paclitaxel (6)	-26	0 (0%)	EDTA	4:21	5	25
OC7	III	Carboplatin/paclitaxel (Neoadj) (3)	11	0 (0%)	EDTA	23:02	5	-
OC8	III	Cisplatin/pegylated liposomal doxorubicin (Neoadj) (4)	-22	0 (0%)	Streck	19:15	4.5	-
OC9	III	Cisplatin/gemcitabine (6)	-196	0 (0%)	EDTA	2:23	5	-
OC10	IIIc	Carboplatin/paclitaxel (6)	-109	1 (100%)	EDTA	23:04	5	-

**Table 2.** Blood collections and timings. *N/A* not assessable. \*Time between blood collection and tissue biopsy. \*CR—no residual tumour tissue at interval debulking. <sup>^</sup>Ascites noted after debulking.

of *TP53* mutations. Possibly future studies should concurrently sequence matched ctDNA and peripheral blood mononuclear cells to eliminate mutations associated with CHIP.

Previous studies have suggested that disease evolution impose somatic mutational landscape changes, which is an important consideration when selecting mutations for longitudinal patient monitoring. A significant caveat of this study was the long gap between blood collection and tumour tissue sampling in the majority of patients (Table 2). Thus, the discordance of the mutational profile may be attributed to clonal evolution in the intervening period between plasma ctDNA isolation and tissue biopsy. Other studies assessing NGS or digital PCR approaches for HGSOc prior to therapy have shown that ctDNA is readily detectable using *TP53*<sup>25–27</sup>, even as early as stage I<sup>27</sup>. Furthermore, ctDNA dynamics during treatment, particularly poor reduction of ctDNA levels, are capable of predicting worse outcomes<sup>25,26</sup>, indicating the clinical utility of ctDNA in HGSOc management.

Overall, our study demonstrates the utility of a UMI-tagged NGS panel for plasma *TP53* mutation screening in HGSOc patients. Further studies will need to address if this methodology will be suitable for measuring residual disease and response to therapy.

## Data availability

Data available upon reasonable request to the corresponding authors, Elin Gray, e.gray@ecu.edu.au.

Received: 31 January 2022; Accepted: 2 January 2023

Published online: 06 January 2023

## References

- Soletormos, G. *et al.* Clinical use of cancer biomarkers in epithelial ovarian cancer: Updated guidelines from the European Group on tumor markers. *Int. J. Gynecol. Cancer* **26**, 43–51. <https://doi.org/10.1097/igc.0000000000000586> (2016).
- Sturgeon, C. M. *et al.* National Academy of Clinical Biochemistry Laboratory medicine practice guidelines for use of tumor markers in testicular, prostate, colorectal, breast, and ovarian cancers. *Clin. Chem.* **54**, e11–e79. <https://doi.org/10.1373/clinchem.2008.105601> (2008).
- Saygili, U., Guclu, S., Uslu, T., Erten, O. & Dogan, E. The effect of ascites, mass volume, and peritoneal carcinomatosis on serum CA125 levels in patients with ovarian carcinoma. *Int. J. Gynecol. Cancer* **12**, 438–442 (2002).
- Diehl, F. *et al.* Circulating mutant DNA to assess tumor dynamics. *Nat. Med.* **14**, 985–990. <https://doi.org/10.1038/nm.1789> (2008).
- To, E. W. *et al.* Rapid clearance of plasma Epstein–Barr virus DNA after surgical treatment of nasopharyngeal carcinoma. *Clin. Cancer Res.* **9**, 3254–3259 (2003).
- The Cancer Genome Atlas Research Network. Integrated genomic analyses of ovarian carcinoma. *Nature* **474**, 609–615. <https://doi.org/10.1038/nature10166> (2011).
- Ahmed, A. A. *et al.* Driver mutations in *TP53* are ubiquitous in high grade serous carcinoma of the ovary. *J. Pathol.* **221**, 49–56. <https://doi.org/10.1002/path.2696> (2010).
- Kobel, M. *et al.* Optimized p53 immunohistochemistry is an accurate predictor of *TP53* mutation in ovarian carcinoma. *J. Pathol. Clin. Res.* **2**, 247–258. <https://doi.org/10.1002/cjp.2.53> (2016).
- Forshe, T. *et al.* Noninvasive identification and monitoring of cancer mutations by targeted deep sequencing of plasma DNA. *Sci. Transl. Med.* **4**, 136–168. <https://doi.org/10.1126/scitranslmed.3003726> (2012).
- Otsuka, J. *et al.* Detection of p53 mutations in the plasma DNA of patients with ovarian cancer. *Int. J. Gynecol. Cancer* **14**, 459–464. <https://doi.org/10.1111/j.1048-891x.2004.014305.x> (2004).
- Pereira, E. *et al.* Personalized circulating tumor DNA biomarkers dynamically predict treatment response and survival in gynecologic cancers. *PLoS ONE* **10**, e0145754. <https://doi.org/10.1371/journal.pone.0145754> (2015).
- Swisher, E. M. *et al.* Tumor-specific p53 sequences in blood and peritoneal fluid of women with epithelial ovarian cancer. *Am. J. Obstet. Gynecol.* **193**, 662–667. <https://doi.org/10.1016/j.ajog.2005.01.054> (2005).



13. Calapre, L. *et al.* Locus-specific concordance of genomic alterations between tissue and plasma circulating tumor DNA in metastatic melanoma. *Mol. Oncol.* **13**, 171–184. <https://doi.org/10.1002/1878-0261.12391> (2019).
14. Cai, X., Janku, F., Zhan, Q. & Fan, J. B. Accessing genetic information with liquid biopsies. *Trends Genet.* **31**, 564–575. <https://doi.org/10.1016/j.tig.2015.06.001> (2015).
15. Crowley, E., Di Nicolantonio, F., Loupakis, F. & Bardelli, A. Liquid biopsy: Monitoring cancer-genetics in the blood. *Nat. Rev. Clin. Oncol.* **10**, 472–484. <https://doi.org/10.1038/nrclinonc.2013.110> (2013).
16. Kivioja, T. *et al.* Counting absolute numbers of molecules using unique molecular identifiers. *Nat. Methods* **9**, 72. <https://doi.org/10.1038/nmeth.1778> (2011).
17. Diaz, L. A. Jr. & Bardelli, A. Liquid biopsies: Genotyping circulating tumor DNA. *J. Clin. Oncol.* **32**, 579–586. <https://doi.org/10.1200/jco.2012.45.2011> (2014).
18. Vanderstichele, A. *et al.* Chromosomal instability in cell-free DNA as a highly specific biomarker for detection of ovarian cancer in women with adnexal masses. *Clin. Cancer Res.* **23**, 2223. <https://doi.org/10.1158/1078-0432.CCR-16-1078> (2017).
19. Vitale, S. R. *et al.* TP53 mutations in serum circulating cell-free tumor DNA as longitudinal biomarker for high-grade serous ovarian cancer. *Biomolecules* **10**, 30415. <https://doi.org/10.3390/biom10030415> (2020).
20. Paracchini, L. *et al.* Genome-wide copy-number alterations in circulating tumor DNA as a novel biomarker for patients with high-grade serous ovarian cancer. *Clin. Cancer Res.* **27**, 2549–2559. <https://doi.org/10.1158/1078-0432.Ccr-20-3345> (2021).
21. Jaiswal, S. *et al.* Age-related clonal hematopoiesis associated with adverse outcomes. *N. Engl. J. Med.* **371**, 2488–2498. <https://doi.org/10.1056/NEJMoa1408617> (2014).
22. Liu, J. *et al.* Biological background of the genomic variations of cf-DNA in healthy individuals. *Ann. Oncol.* **30**, 464–470. <https://doi.org/10.1093/annonc/mdy513> (2019).
23. Razavi, P. *et al.* High-intensity sequencing reveals the sources of plasma circulating cell-free DNA variants. *Nat. Med.* **25**, 1928–1937. <https://doi.org/10.1038/s41591-019-0652-7> (2019).
24. Hu, Y. *et al.* False-positive plasma genotyping due to clonal hematopoiesis. *Clin. Cancer Res.* **24**, 4437. <https://doi.org/10.1158/1078-0432.CCR-18-0143> (2018).
25. Kim, Y. M. *et al.* Prospective study of the efficacy and utility of TP53 mutations in circulating tumor DNA as a non-invasive biomarker of treatment response monitoring in patients with high-grade serous ovarian carcinoma. *J. Gynecol. Oncol.* **30**, e32. <https://doi.org/10.3802/jgo.2019.30.e32> (2019).
26. Parkinson, C. A. *et al.* Exploratory analysis of TP53 mutations in circulating tumour DNA as biomarkers of treatment response for patients with relapsed high-grade serous ovarian carcinoma: A retrospective study. *PLoS Med.* **13**, e1002198. <https://doi.org/10.1371/journal.pmed.1002198> (2016).
27. Noguchi, T. *et al.* Comprehensive gene mutation profiling of circulating tumor DNA in ovarian cancer: Its pathological and prognostic impact. *Cancers (Basel)* **12**, 113382. <https://doi.org/10.3390/cancers12113382> (2020).

## Acknowledgements

The authors thank all the participants, patients, and healthy volunteers, for their assistance with the study. The authors would also like to thank Dr Cristian Ionescu-Zanetti and Dr Jeff Jensen from Fluxion Biosciences for their expertise in Erase-seq. ESG is supported by a Fellowship from the Cancer Council of Western Australia.

## Author contributions

L.C., T.M.M., B.A. and E.S.G. designed the study; L.C., T.G., A.B.B., A.L.R. carried out experiments; T.M.M. recruited patients and collect clinical information; C.S. and B.A. reviewed pathology samples; L.C. analysed data and wrote the manuscript; E.S.G. supervised the study; all authors reviewed the final manuscript.

## Competing interests

The authors declare no competing interests.

## Additional information

**Supplementary Information** The online version contains supplementary material available at <https://doi.org/10.1038/s41598-023-27445-2>.

**Correspondence** and requests for materials should be addressed to E.S.G.

**Reprints and permissions information** is available at [www.nature.com/reprints](http://www.nature.com/reprints).

**Publisher's note** Springer Nature remains neutral with regard to jurisdictional claims in published maps and institutional affiliations.



**Open Access** This article is licensed under a Creative Commons Attribution 4.0 International License, which permits use, sharing, adaptation, distribution and reproduction in any medium or format, as long as you give appropriate credit to the original author(s) and the source, provide a link to the Creative Commons licence, and indicate if changes were made. The images or other third party material in this article are included in the article's Creative Commons licence, unless indicated otherwise in a credit line to the material. If material is not included in the article's Creative Commons licence and your intended use is not permitted by statutory regulation or exceeds the permitted use, you will need to obtain permission directly from the copyright holder. To view a copy of this licence, visit <http://creativecommons.org/licenses/by/4.0/>.

© The Author(s) 2023